DNA Nanostructures **Hot Paper**

One-Step Formation of "Chain-Armor"-Stabilized DNA Nanostructures**

Valentina Cassinelli, Birgit Oberleitner, Jessica Sobotta, Philipp Nickels, Guido Grossi, Susanne Kempter, Thomas Frischmuth, Tim Liedl, and Antonio Manetto

Abstract: *DNA-based self-assembled nanostructures are widely used to position organic and inorganic objects with nanoscale precision. A particular promising application of DNA structures is their usage as programmable carrier systems for targeted drug delivery. To provide DNA-based templates that are robust against degradation at elevated temperatures, low ion concentrations, adverse pH conditions, and DNases, we built 6-helix DNA tile tubes consisting of 24 oligonucleotides carrying alkyne groups on their 3'-ends and azides on their 5'-ends. By a mild click reaction, the two ends of selected oligonucleotides were covalently connected to form rings and interlocked DNA single strands, so-called DNA catenanes. Strikingly, the structures stayed topologically intact in pure water and even after precipitation from EtOH. The structures even withstood a temperature of 95°C when all of the 24 strands were chemically interlocked.*

The multidisciplinary field of DNA nanotechnology, introduced theoretically[1] and practically[2] by Seeman, opened the route to the synthesis of structures of unprecedented precision at the nanometer scale. Today, DNA origami[3] and the single-stranded tile method (SST)[4] are routinely used to self-assemble complex nanostructures for various potential applications.[5] For example, the use of nanosystems for biomedical and diagnostic purposes lead to approaches for cellular immunostimulation,[6] controlled drug delivery to cells,[7] vaccine design and synthesis,[8] and membrane channel assembly.[9] Nevertheless, in most biological applications, DNA nanostructures are exposed to conditions that have adverse effects on Watson–Crick base pairing and can lead to the untimely dissociation of DNA double strands. Cell media, for example, often have concentrations of divalent cations below 2 mM, which is an order of magnitude lower than Mg^{2+} concentrations used in most assembly protocols for DNA structures. Recent studies showed that low concentrations of divalent cations in combination with temperatures higher than 35°C are enough to cause the disassembly of a range of DNA objects within 24 h or less.[10] A common method to increase the stability of DNA towards nuclease degradation relies on the incorporation of nonnatural bases or backbones. However, to maintain topological integrity, covalent linkage of the DNA bases is desirable. In the past years there have been reports on the moderately elevated thermal resistance of DNA origami structures resulting from the random photo-crosslinking of DNA strands with 8-methoxypsoralen[11] and interlocked DNA and RNA nanostructures including two- to five-membered catenanes,[12] borromean rings,[13] and trefoil and other knots[14] from single-stranded and double-stranded nucleic acids.[15] However, the artificial assembly of catenated structures containing more than five DNA rings or even more complex systems such as the chain-armor-like DNA found in certain single-cell flagellate protozoa (trypanosomatids)[16] remained challenging.[17] Nevertheless, such large DNA catenanes are of interest for future DNA nanotechnology applications such as biomedicine in which tolerance to denaturing conditions is indispensable. Here we report the use of SST DNA nanotubes combined with the highly efficient click chemistry method for the efficient and one-pot stoichiometric assembly of DNA catenanes to an unprecedented complexity of up to 24 DNA rings. Our results demonstrate stoichiometric synthesis of "chain-armor" DNA with almost quantitative yields.

SST assembly is a modular and reliable method to fold two- and three-dimensional DNA nanoarchitectures from synthetic oligonucleotides.[18] We here used a six-helix bundle[19] hereinafter called 6-helix tube (6HT) consisting of 24 oligonucleotides (Scheme 1). To achieve the formation of DNA catenanes, selected neighboring strands of the 6HT were replaced by (3'-alkyne,5'-azide)-modified oligonucleotides hereinafter called click tiles (Scheme 1a) giving rise to

[*] V. Cassinelli, Dr. B. Oberleitner, J. Sobotta, Dr. T. Frischmuth, Dr. A. Manetto
baseclick GmbH
Bahnhofstrasse 9–15, 82327 Tutzing (Germany)
E-mail: a.manetto@baseclick.eu

V. Cassinelli
Department Chemistry and Biochemistry
Ludwig-Maximilians-Universität (LMU)
Butenandtstrasse 5-13, 81377 Munich (Germany)

J. Sobotta
Department Applied Chemistry
Technische Hochschule Nürnberg G. S. Ohm
Kesslerplatz 12, 90489 Nürnberg (Germany)

P. Nickels, Dr. S. Kempter, Prof. T. Liedl
Physics Department and CeNS
Ludwig-Maximilians-Universität (LMU)
Geschwister-Scholl-Platz 1, 80539 Munich (Germany)

G. Grossi
Interdisciplinary Nanoscience Center (iNANO)
Aarhus University
Gustav Wieds Vej 14, 8000 Aarhus (Denmark)
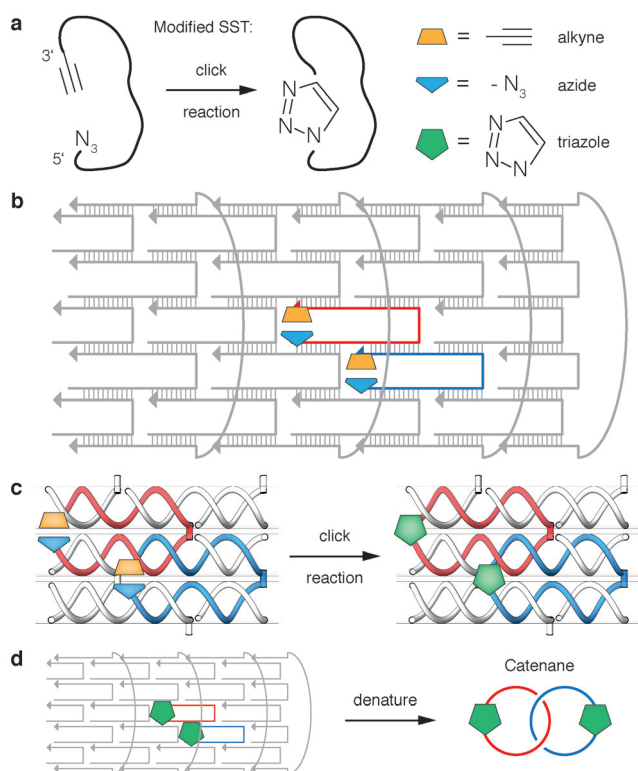
Scheme 1. Graphical representation of the click reaction (a) occurring in the DNA nanotube (b,c) in a preorganized fashion yielding a DNA catenane (d)

modified tubes (MX-tube with X = number of click tiles included into the structure). The intramolecular cyclization is facilitated by the preorganization within the folded tube. Moreover, if two or more intertwined click tiles are present, the simultaneous intramolecular cyclization results in the formation of topologically interlocked ssDNA (Scheme 1b–d). The reaction between alkyne and azide groups catalyzed by copper(I) ions (copper-catalyzed azide–alkyne cycloaddition, CuAAC)[20] is here the enabling factor, with CuAAC being the most prominent example of click chemistry[21] due to the high reactivity of its components along with their chemical stability, commercial availability, and bio-orthogonality towards, for example, nucleic acids.[22]

We first introduced two click tiles, each 42-mers, within the 6HT structure to obtain an M2 tube (Scheme 1b). Native agarose gel analysis (2%, 1 × TE, 11 mM $MgCl_2$) of the folded M2 tube revealed no detectable shift of the band with respect to the unmodified 6HT tube along with comparable folding yields of up to 90%. Transmission electron microscopy (TEM) imaging confirmed the correct folding of both structures. Click reagents (baseclick GmbH, Germany) were then added to both unmodified 6HT and modified M2 tubes and a series of click reaction conditions were tested. In accordance with published data,[23] the click reagents did not damage the folded structure nor did they influence the electrophoretic properties of unmodified 6HT and modified M2 tubes even after several hours of reaction at temperatures between 4°C and 45°C.

To investigate whether the formation of the two rings within the M2 tube after the click reaction was successful, both unmodified 6HT and modified M2 tubes before and after the click reaction were analyzed by RP-HPLC and LC-MS (see the Supporting Information) and denaturing polyacrylamide gel electrophoresis (PAGE). For the unmodified tubes and M2 tubes before the click reaction, only low-molecular-weight bands below the 50-mer ladder were visible and could be assigned to the individual strands (Figure 1a). As anticipated, only the modified M2 tube after click reaction—marked as M2* tube—showed a clear band migrating at roughly 100 bp. This band was assigned to a newly formed 84-mer heterodimer (Scheme 1d). Each ring consists of an oligonucleotide covalently connected at its ends via a triazole moiety resulting from the intramolecular CuAAC between the 5′-azide group and the 3′-alkyne group of the oligonucleotide. The preorganization of these two modified strands within the tube ensures the regioselectivity of this reaction: the reactive groups of one oligonucleotide are one helix turn (3.4 nm) away from those present in the second modified strand. To support this hypothesis, a free azide was added as competitor to the click reaction mixture along with the M2 tube. The band assigned to the two-membered ring persisted even though the competitor was present in high molar excess (Figure S15).

To explore whether our approach can be extended to the synthesis of multiring DNA catenanes, we designed four more six-helix tubes each containing a different number of click
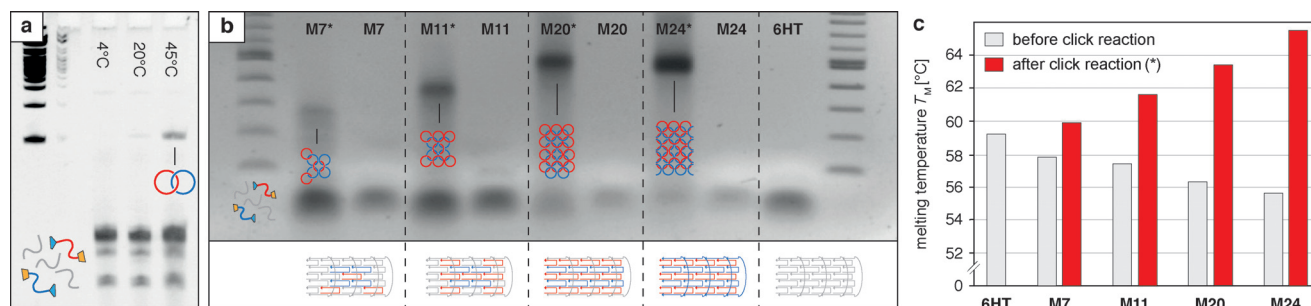

Figure 1. a) 10% denaturing PAGE analysis of 6HT containing two azide-/alkyne-modified (M2) strands ("M2 tubes") after 1.5 h click reaction at 4°C, 20°C, and 45°C (see also Figure S10). b) Native 2% agarose gel electrophoresis lacking $MgCl_2$ of tubes containing an increasing number of click tiles. Modified tubes after the click reaction are identified by an asterisk (M7*–M24*) and show the corresponding DNA catenane band. Untreated tubes (M7–M24 and 6HT) unfold during the gel migration and show only lower-molecular-weight bands of the individual strand. c) Bar diagram of the measured melting temperatures before (gray) and after (red) the click reaction.

tiles, which in keeping with our nomenclature were called M7, M11, M20, and M24 tubes. Modified tubes treated with the click reaction reagents are additionally marked with an asterisk. The introduction of more than two click tiles did not influence the correct folding of the tube as confirmed by TEM imaging, nor did it induce a shift in migration speed in agarose gel analysis (see the Supporting Information). Also, the subsequent click reaction carried out on both unmodified and modified tubes did not result in structural alterations of the assembled tubes.

The presence of salts—preferably containing divalent cations such as Mg^{2+}—is necessary for the stability of DNA nanostructures.[10a] The 6HT used in this study requires 20 mM $MgCl_2$ to fold correctly and efficiently. When folded DNA nanotubes were analyzed via agarose gels lacking divalent ions, the nanotubes unfolded and only the individual strands were observed as low-molecular-weight bands. This principle was used to investigate the assembly and stability of the modified tubes M7*, M11*, M20*, and M24* resulting from click reaction. As expected, both unmodified 6HT and tubes before the click reaction disassembled completely (Figure 1b) and tubes after the click reaction showed slower migrating bands corresponding to the interlocked catenanes. Remarkably, almost no fast migrating band of individual strands was visible in the lane with the M24* tube, which demonstrates the efficacy of this one-pot stoichiometric multicyclization reaction.[24] This result was further confirmed by an extra set of experiments involving fluorescent labeled click tiles. Strikingly, similar results were obtained when the catenane-containing nanostructures were heated to 95°C and then loaded on the gel or after EtOH precipitation of the nanostructures (see the Supporting Information).

In a next step, the melting transitions of the tubes were measured using a fluorimetric assay with DNA intercalating dyes:[25] melting temperatures decreased with higher amounts of click tiles before the reaction while an increasing melting temperature was recorded for tubes with more closed rings (cyclized strands) (Figure 1c). Compared to the unmodified 6HT, a decrease of 3.6°C was measured when all 24 strands of the tube were substituted with the corresponding click tiles, which may be due to an energy penalty resulting from the incorporation of the alkyne and azide groups into the DNA structure. If, on the other hand, the click reaction is performed and the catenanes are formed, the melting temperature increases by 6.3°C for the 24-ring structure. This effect could be attributed to the increased local concentration of the partnering DNA sequences in the catenanes. We expected that the M24* tube would remain a monodisperse, covalently locked macromolecule when exposed to stringent denaturing conditions. To corroborate this hypothesis, samples 6HT, M24, and M24* were desalted after regular folding using nitrocellulose membranes. Subsequently, all samples were analyzed in agarose gels. Only the M24* tube survived the desalting process and appeared as a clear band migrating at the correct speed (Figure 2a).

Additionally, we also exposed the tubes to "Dulbecco's Modified Eagle Medium" (DMEM, Merck-Millipore) and incubated them for 24 h at 37°C. Under these conditions, the M24* tube persisted as a monodisperse nanostructure while
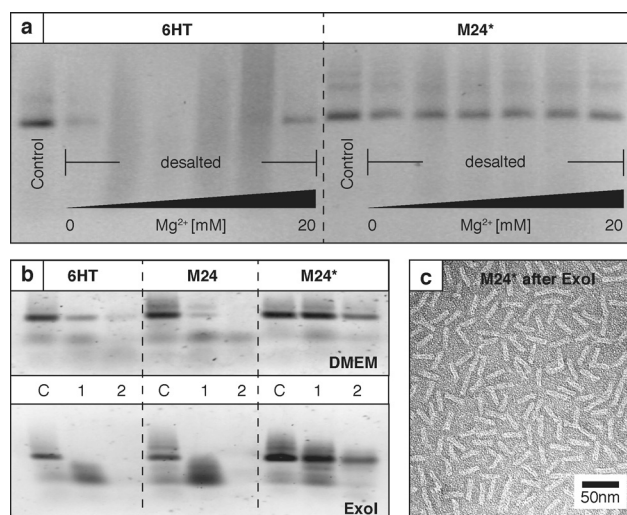

Figure 2. a) Native agarose gel (2%, 1×TE/MgCl$_2$) of 6HT (left) and M24* (right) equilibrated via microdialysis with ddH$_2$O ([Mg^{2+}]=0) or 1×TE buffer containing 0.1, 1, 5, 10, and 20 mM MgCl$_2$. b) Agarose gels (2%, 1×TE/MgCl$_2$) of 6HT, M24, and M24*. Top: C=control; 1=24 h at 37°C; 2=24 h at 37°C in DMEM. Bottom: C=control; 1=15 min at 65°C; 2=15 min at 65°C, then treated with exonuclease I for 3 h at 37°C. c) TEM image of M24* denatured at 65°C and submitted to 3 h Exo I digestion.

the M24 tube and the unmodified 6HT unfolded completely. (Figure 2b, top). To further test the stability, the samples were incubated at 65°C for 15 min, cooled in ice water, and submitted to exonuclease I (Exo I, Thermo Scientific, 10 units) digestion at 37°C for 3 h. The M24* tubes remained intact after this treatment and appeared as a defined band in the native agarose gel (Figure 2b, bottom). TEM imaging of these samples revealed well-defined tubes of the expected size (Figure 2c).

The presented cyclization of DNA strands via click reaction resulted in the efficient formation of interlocked single-stranded rings due to the spatial preorganization of the reactive groups in a SST assembly. Our method constitutes, to our knowledge, the first example of a one-pot stoichiometry-controlled reaction to form multiring DNA catenanes and of "chain-armor" tubes. The resulting increased resistance of such "chain-armor" DNA structures to low cation concentrations, high temperatures, and exonuclease activity could solve stability issues of DNA structures in in vitro and in vivo applications. The method is not limited to the production of DNA catenanes of varying sizes and chain geometries but could be further applied to assemble oligonucleotides for the synthesis of long single-stranded DNA, thus paving the way to a non-enzymatic approach to gene synthesis.

Experimental Section

Oligonucleotides used in this work have two different lengths: 18 42-mer strands form the center region and 6 28-mer strands form the two ends of the tube (Scheme 1b). All tubes were folded by cooling a buffer solution (1×TE, 20 mM MgCl$_2$) containing n click tiles and $24-n$ unmodified strands ($n=0, 2, …, 24$) from 80°C to 65°C in steps of 1°Cmin^{-1} followed by a slower ramp from 65°C to 25°C in steps of

0.5°C every 12 min. Details on click chemistry, HPLC analysis, stability assays are provided in the Supporting Information.

[1] N. C. Seeman, *J. Theor. Biol.* **1982**, *99*, 237–247.
[2] a) J. Chen, N. C. Seeman, *Nature* **1991**, *350*, 631–633; b) T. J. Fu, N. C. Seeman, *Biochemistry* **1993**, *32*, 3211–3220; c) E. Winfree, F. Liu, L. A. Wenzler, N. C. Seeman, *Nature* **1998**, *394*, 539–544.
[3] P. W. K. Rothemund, *Nature* **2006**, *440*, 297–302.
[4] a) Y. Ke, L. L. Ong, W. M. Shih, P. Yin, *Science* **2012**, *338*, 1177–1183; b) B. Wei, M. Dai, P. Yin, *Nature* **2012**, *485*, 623–626.
[5] a) N. C. Seeman, *Annu. Rev. Biochem.* **2010**, *79*, 65–87; b) D. Smith, V. Schüller, C. Engst, J. Rädler, T. Liedl, *Nanomedicine* **2013**, *8*, 105–121; c) M. Endo, Y. Yang, H. Sugiyama, *Biomater. Sci.* **2013**, *1*, 347–360.
[6] a) J. Li, H. Pei, B. Zhu, L. Liang, M. Wei, Y. He, N. Chen, D. Li, Q. Huang, C. Fan, *ACS Nano* **2011**, *5*, 8783–8789; b) V. J. Schüller, S. Heidegger, N. Sandholzer, P. C. Nickels, N. A. Suhartha, S. Endres, C. Bourquin, T. Liedl, *ACS Nano* **2011**, *5*, 9696–9702.
[7] a) S. M. Douglas, I. Bachelet, G. M. Church, *Science* **2012**, *335*, 831–834; b) Q. Jiang, C. Song, J. Nangreave, X. Liu, L. Lin, D. Qiu, Z.-G. Wang, G. Zou, X. Liang, H. Yan, et al., *J. Am. Chem. Soc.* **2012**, *134*, 13396–13403; c) H. Lee, A. K. R. Lytton-Jean, Y. Chen, K. T. Love, A. I. Park, E. D. Karagiannis, A. Sehgal, W. Querbes, C. S. Zurenko, M. Jayaraman, et al., *Nat. Nano* **2012**, *7*, 389–393; d) A. S. Walsh, H. Yin, C. M. Erben, M. J. A. Wood, A. J. Turberfield, *ACS Nano* **2011**, *5*, 5427–5432; e) Y.-X. Zhao, A. Shaw, X. Zeng, E. Benson, A. M. Nyström, B. Högberg, *ACS Nano* **2012**, *6*, 8684–8691.
[8] X. Liu, Y. Xu, T. Yu, C. Clifford, Y. Liu, H. Yan, Y. Chang, *Nano Lett.* **2012**, *12*, 4254–4259.
[9] M. Langecker, V. Arnaut, T. G. Martin, J. List, S. Renner, M. Mayer, H. Dietz, F. C. Simmel, *Science* **2012**, *338*, 932–936.
[10] a) J. Hahn, S. F. J. Wickham, W. M. Shih, S. D. Perrault, *ACS Nano* **2014**, *8*, 8765–8775; b) S. D. Perrault, W. M. Shih, *ACS Nano* **2014**, *8*, 5132–5140; c) S. Kocabey, H. Meinl, I. S. MacPherson, V. Cassinelli, A. Manetto, S. Rothenfusser, T. Liedl, F. S. Lichtenegger, *Nanomaterials* **2015**, *5*, 47–60.
[11] A. Rajendran, M. Endo, Y. Katsuda, K. Hidaka, H. Sugiyama, *J. Am. Chem. Soc.* **2011**, *133*, 14488–14491.
[12] R. P. Goodman, I. A. T. Schaap, C. F. Tardin, C. M. Erben, R. M. Berry, C. F. Schmidt, A. J. Turberfield, *Science* **2005**, *310*, 1661.
[13] C. Mao, W. Sun, N. C. Seeman, *Nature* **1997**, *386*, 137–138.
[14] a) S. M. Du, N. C. Seeman, *Biopolymers* **1994**, *34*, 31–37; b) S. M. Du, B. D. Stollar, N. C. Seeman, *J. Am. Chem. Soc.* **1995**, *117*, 1194–1200.
[15] a) S. S. Jester, M. Famulok, *Acc. Chem. Res.* **2014**, *47*, 1700–1709; b) T. Li, F. Lohmann, M. Famulok, *Nat. Commun.* **2014**, *5*, 4940; c) F. Lohmann, J. Valero, M. Famulok, *Chem. Commun.* **2014**, *50*, 6091–6093; d) T. L. Schmidt, A. Heckel, *Nano Lett.* **2011**, *11*, 1739–1742.
[16] a) J. Chen, C. A. Rauch, J. H. White, P. T. Englund, N. R. Cozzarelli, *Cell* **1995**, *80*, 61–69; b) B. Liu, Y. Liu, S. A. Motyka, E. E. C. Agbo, P. T. Englund, *Trends Parasitol.* **2005**, *21*, 363–369.
[17] C. H. Lu, X. J. Qi, A. Cecconello, S. S. Jester, M. Famulok, I. Willner, *Angew. Chem. Int. Ed.* **2014**, *53*, 7499–7503; *Angew. Chem.* **2014**, *126*, 7629–7633.
[18] Y. Ke, L. L. Ong, W. Sun, J. Song, M. Dong, W. M. Shih, P. Yin, *Nat. Chem.* **2014**, *6*, 994–1002.
[19] F. Mathieu, S. Liao, C. Mao, J. Kopatsch, T. Wang, N. C. Seeman, *Nano Lett.* **2005**, *5*, 661–665.
[20] a) V. V. Rostovtsev, L. G. Green, V. V. Fokin, K. B. Sharpless, *Angew. Chem. Int. Ed.* **2002**, *41*, 2596–2599; *Angew. Chem.* **2002**, *114*, 2708–2711; b) C. W. Tornøe, C. Christensen, M. Meldal, *J. Org. Chem.* **2002**, *67*, 3057–3064.
[21] H. C. Kolb, M. G. Finn, K. B. Sharpless, *Angew. Chem. Int. Ed.* **2001**, *40*, 2004–2021; *Angew. Chem.* **2001**, *113*, 2056–2075.
[22] P. M. E. Gramlich, C. T. Wirges, A. Manetto, T. Carell, *Angew. Chem. Int. Ed.* **2008**, *47*, 8350–8358; *Angew. Chem.* **2008**, *120*, 8478–8487.
[23] N. V. Voigt, T. Torring, A. Rotaru, M. F. Jacobsen, J. B. Ravnsbaek, R. Subramani, W. Mamdouh, J. Kjems, A. Mokhir, F. Besenbacher, K. V. Gothelf, *Nat. Nanotechnol.* **2010**, *5*, 200–203.
[24] Interstrand click reactions cannot be excluded for the three terminal click tiles (J1S1, J3S1, and J5S1; left side of Figure S3) due to the particular design of this tube. Experimental observations support the formation of small amounts of interstrand side products. Anyway, the overall stability of this particular design is not affected by interstrand reactions.
[25] T. L. Sobey, S. Renner, F. C. Simmel, *J. Phys. Condens. Matter* **2009**, *21*, 034112.